https://doi.org/10.31436/iiumej.v27i1.3980

Surrogate Model-based Optimization of a Biplane Unmanned Aerial Vehicle Wing Using Genetic Algorithm and Response Surface Methodology

YUKSEL ERASLAN*

Aerospace Engineering Department, Tarsus University, Mersin, Türkiye

**Corresponding author: yukseleraslan@tarsus.edu.tr*

(Received: 10 October 2025; Accepted: 20 December 2025; Published online: 12 January 2026)

ABSTRACT: Multi-wing aerial vehicle designs have existed since the early days of aviation; however, they are not commonly employed in modern designs, as advances in materials technology have enabled the structurally feasible high-aspect-ratio monoplane configurations. Nevertheless, the application has the potential to serve as a solution in the field of mini unmanned aerial vehicle (UAV) design, offering the advantage of a smaller wing span. The most popular multi-wing application, the biplane, features two wings mounted in parallel and is typically characterized by the geometric terms decalage, stagger, and gap, which should be optimized during the design process. This study focuses on aerodynamic optimization of a biplane wing to maximize the lift-to-drag ratio (C_L/C_D) and the $C_L^{3/2}/C_D$ by optimizing the aforementioned geometric parameters. To this end, the aerodynamic analysis method was initially validated by comparing it with wind-tunnel data for a monoplane wing reported in the literature. The Response Surface Method (RSM) was used to assess the effects of the design parameters and to generate surrogate models for C_L/C_D and $C_L^{3/2}/C_D$. The optimal design was determined using the genetic algorithm. The results indicated that decalage and gap distance primarily determine range improvement, whereas gap and stagger are the primary parameters for improving endurance. The applied optimization approach resulted in improvements of 10.93% in range and 46.63% in endurance relative to the base biplane configuration.

ABSTRAK: Reka bentuk kenderaan udara berbilang sayap telah wujud sejak awal perkembangan penerbangan; namun, ia jarang digunakan dalam reka bentuk moden berikutan kemajuan teknologi bahan yang membolehkan nisbah-aspek-tinggi konfigurasi monosayap lebih berdaya struktur. Namun, aplikasi berbilang sayap berpotensi menjadi penyelesaian reka bentuk kenderaan udara tanpa pemandu bersaiz kecil (mini UAV), khususnya dengan kelebihan bentangan sayap lebih kecil. Konfigurasi berbilang sayap iaitu paling lazim, sayap berkembar (biplane), merujuk kepada dua sayap yang disusun selari dan dicirikan oleh parameter geometri utama seperti sela, aturan, dan jurang, perlu ditentukan secara optimum dalam proses reka bentuk. Kajian ini memfokuskan kepada pengoptimuman aerodinamik sayap berkembar bagi memaksimumkan nisbah angkat kepada seretan (C_L/C_D) dan $C_L^{3/2}/C_D$ melalui pemilihan optimum parameter geometri tersebut. Kaedah analisis aerodinamik terlebih dahulu disahkan melalui perbandingan data terowong angin bagi monosayap yang dilaporkan dalam literatur. Kaedah Permukaan Tindak Balas (Response Surface Method, RSM) digunakan bagi menilai kesan parameter reka bentuk dan model pengganti bagi C_L/C_D dan $C_L^{3/2}/C_D$, manakala reka bentuk optimum ditentukan menggunakan algoritma genetik. Keputusan menunjukkan bahawa sela dan jurang merupakan parameter utama dalam peningkatan jarak terbang, manakala jurang dan aturan lebih dominan dalam meningkatkan daya tahan penerbangan. Pendekatan pengoptimuman yang dicadangkan menghasilkan

peningkatan sebanyak 10.93% dari segi jarak dan 46.63% dari segi daya tahan berbanding konfigurasi sayap berkembar asas.

KEYWORDS: *Biplane, UAV, Response surface method, Aerodynamic optimization, Genetic algorithm.*

1. INTRODUCTION

The first attempts at multi-wing aerial vehicle designs date back to the early 20th century, from the Wright Brothers' "Wright Flyer" in 1903. The most common multiple-wing configurations are the biplane and triplane, which are designated by the number of nonplanar wings. Today, the prevalence of these designs has diminished with advancements in materials science and, correspondingly, improvements in the aerodynamic efficiency of monoplanes [1]. Modern fixed-wing UAV designs commonly feature a single, often large, wing intended to be both lightweight and sufficiently structurally rigid to withstand aerodynamic loads, which presents a complex engineering challenge. Instead, multi-wing configurations could be a useful alternative, offering the advantage of distributing the required wing area across multiple shorter wings. Such a design is advantageous for operations such as indoor inspection, navigating dense urban canyons for delivery services, search-and-rescue operations after natural disasters involving collapsed structures, and close-proximity environmental monitoring in forests or industrial facilities. Furthermore, the reduced wingspan could also provide a lower moment of inertia and improved manoeuvrability by shifting the centre of wing mass closer to the longitudinal axis.

The presence of an additional wing in proximity significantly alters the pressure distribution and flow patterns around the wings. The increased aerodynamic interference leads to a reduction in the effective angle of attack, a change in lift distribution, an increase in induced drag, and an overall decrease in aerodynamic efficiency for multi-wings when compared with a monoplane generating equal lift. To enhance the aerodynamic performance of a biplane configuration, the wing arrangement is critical. The geometrical parameters of decalage, stagger, and gap interact sensitively, necessitating a meticulous design process to achieve optimal aerodynamic performance metrics such as C_L/C_D or $C_L^{3/2}/C_D$ for multi-wings [2, 3]. These parameters have a key role in the range and endurance of a piston-propelled aerial vehicle. In this context, the Response Surface Methodology (RSM) is an appropriate Design of Experiments (DoE) approach for this task, as it can model and analyse relationships among multiple input variables and output responses. Furthermore, the method facilitates the generation of precise surrogate models with fewer computationally expensive simulations than traditional approaches. The generated surrogate model could be integrated into any well-suited optimization algorithm to obtain an optimal design.

In the scientific literature, Design of Experiments (DoE) and Response Surface Methodology (RSM) have been widely used to develop surrogate models for aerospace optimization. A significant number of existing studies focus on fundamental two-dimensional component optimization. Leifsson et al. [4], Immonen [5], and Kallath et al. [10] demonstrated the efficiency of RSM in optimizing airfoil shapes. However, the effectiveness of these optimizations often depends critically on the parametrization technique employed. For instance, while Immonen [5] used a comprehensive set of design candidates, Kallath et al. [10] showed that combining mesh morphing tools with PARSEC definitions enables precise Pareto optimality searches. Furthermore, specific operational environments require tailored DoE approaches. For instance, Win and Thianwiboon [11] successfully applied full factorial designs to capture the unique physics of airfoils in ground effect, highlighting the versatility of standard

DoE methods for constrained flow regimes. On the other hand, three-dimensional wing planforms introduce additional dimensionality, and evolutionary strategies remain popular for global search. For instance, Aelaei et al. [7] and Yao et al. [9] utilized Multi-Objective Genetic Algorithms (MOGA) for delta wings and UAV tail-sitters, respectively. However, recent trends indicate a shift toward gradient-based or hybrid methods to accelerate convergence. Yildirim and Tuncer [12] and Dam et al. [14] demonstrated that coupling surrogate models (such as RSM or Artificial Neural Networks) with Sequential Quadratic Programming (SQP) can efficiently handle parameters like sweep, taper, and twist. Dam et al. [14] noted that ANNs may offer greater flexibility than traditional polynomial-based RSM when training data are abundant.

The literature survey also demonstrated that, in addition to external aerodynamics, advanced surrogate modelling is of critical importance for complex, multidisciplinary interactions. Studies by Tang et al. [6] on turbomachinery and Simmons [13] on distributed propulsion suggest that standard RSM must be enhanced to handle highly non-linear flow physics. Tang et al. [6] addressed this issue by developing a Gradient-Enhanced Response Surface Method (GERSM), proving that incorporating adjoint sensitivity analysis significantly reduces computational cost compared to traditional genetic algorithms. Similarly, applications on Vertical Axis Wind Turbines (VAWT) by Zhang et al. [8] and C-wing configurations by Samputh et al. [15] confirm that robust DoE techniques (such as Orthogonal or Fractional Factorial designs) are essential for isolating the most significant design parameters in complex flow fields.

In summary, the literature review demonstrates that, despite the extensive use of surrogate-based optimization in aerodynamic design, there remains limited literature characterizing the complex interference phenomena associated with biplane UAV configurations. While monoplane planforms have been extensively documented, the impact of coupled variations in gap, stagger, and decalage on flight performance metrics remains to be carefully investigated using modern computational frameworks.

In this context, the present study covers the aerodynamic optimization of a piston-propelled biplane UAV wing by implementing a global optimization strategy utilizing Response Surface Methodology (RSM) and Genetic Algorithms (GA), aiming for achieving maximum lift-to-drag ratio (C_L/C_D) and $C_L^{3/2}/C_D$ by optimal selection of decalage, stagger, and gap distances. The numerical aerodynamic analysis method is validated against wind-tunnel data from the literature, and a surrogate model is developed using RSM to examine the effects of the design parameters on C_L/C_D and $C_L^{3/2}/C_D$. Finally, the surrogate model is used within a genetic algorithm to obtain optimal configurations with respect to decalage, stagger, and gap. The significance of this work lies in substantiating the feasibility of biplane architectures for missions characterised by span constraints and in demonstrating that precise geometric tailoring yields superior performance gains compared with baseline configurations.

2. MATERIAL AND METHOD

2.1. Wing Geometry and Design Parameters

The biplane wing geometry with a 0.4115 *m* wing span, 0.1524 *m* chord length, and Wortmann FX 63-137 airfoil is illustrated in Fig. 1a, where the vertical distance between the upper and lower wing chord lines is denoted as gap (G), a well-known design parameter for multi-wing configurations. The term stagger (S) is the longitudinal distance between the upper and lower wings, and decalage angle (δ) is the relative angle of incidence between the upper and lower wings, as shown in Fig. 1b. The stagger is positive when the upper wing is further

forward than the lower wing, and negative if opposite. The decalage angle can be obtained using Eq. (1).

$$\delta = \theta_u - \theta_l \tag{1}$$

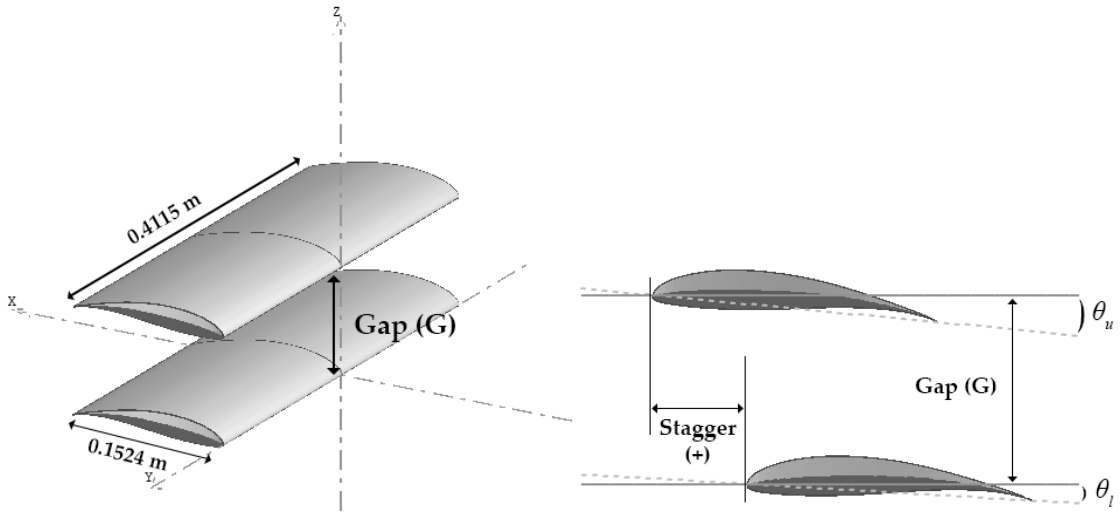

(a) (b)

Figure 1. a) Three-dimensional view and dimensions of the biplane wing,
b) Side view of the biplane wing with stagger, gap, and decalage definitions

2.2. Vortex Lattice Method

The aerodynamic performance of the biplane wing was evaluated using the Vortex Lattice Method (VLM), implemented in the publicly licensed XFLR5 software [16]. The VLM is a standard tool, particularly in the aircraft conceptual design phase, for estimating lift and lift distribution, drag and its components, and moment coefficients. In the VLM, the flow is assumed to be inviscid, incompressible, and irrotational; however, viscous effects can be accounted for using two-dimensional viscous airfoil polars. The wing is divided into a finite number of panels so that the Biot-Savart law can be applied; consequently, the induced velocity and flow tangency are provided at each control point.

To ensure the accuracy of the aerodynamic analysis, the base monoplane wing used in wind-tunnel experiments reported in the literature [17] was analysed over the range -2 to 18 degrees of angle of attack at a Reynolds number of 200,000 and sea-level conditions. The experimental and VLM results were comparatively presented in Fig. 2a and 2b for lift and drag coefficients, respectively. It is clear that, especially at lower angles of attack from -2 to 6 *degrees*, the results were satisfactory within an aircraft conceptual design framework. Moreover, the slopes of the curves are also remarkably promising in both figures, compared with the experimental data. The discrepancy observed between the VLM and the experimental results in the higher-angle-of-attack regime (10 to 15 degrees) is attributed to the well-known limitations of the Vortex Lattice Method. Since the VLM assumes the flow is mainly inviscid, incompressible, and irrotational, viscous effects can be added using two-dimensional viscous airfoil polars. As a result, it accurately predicts aerodynamic coefficients in the linear region (low to moderate angles of attack). However, when the angle of attack exceeds 10 degrees, the flow exhibits significant nonlinear viscous phenomena, including boundary-layer thickening and flow separation (pre-stall conditions). Because the standard VLM formulation does not account for flow separation or complex viscous boundary-layer interactions, it diverges from experimental data in this nonlinear pre-stall regime. As the optimization study primarily targets

the cruise condition (linear region), VLM can be considered sufficiently accurate for conceptual design.

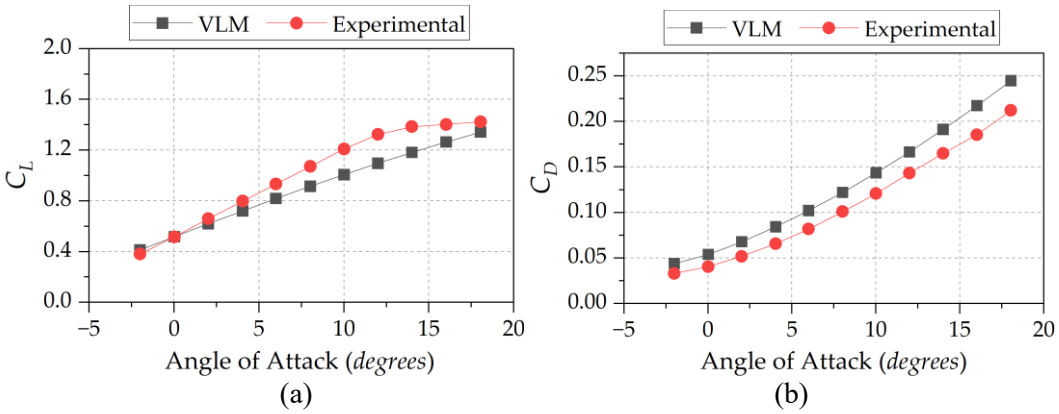

Figure 2. a) The variation in lift coefficient with angle of attack, b) The variation in drag coefficient with angle of attack

The number of panel elements plays a crucial role in panel methods such as VLM. In this context, it varied from 200 to 11,250 to ensure that the results are independent of the number of panels, while the spanwise and chordwise distribution was conserved. The results of analyses at a Reynolds number of 200,000 and sea-level conditions, with a 0-*degree* angle of attack, as shown in Fig. 3, indicate that approximately 4050 elements were sufficient to yield desirable results for both lift and drag coefficients.

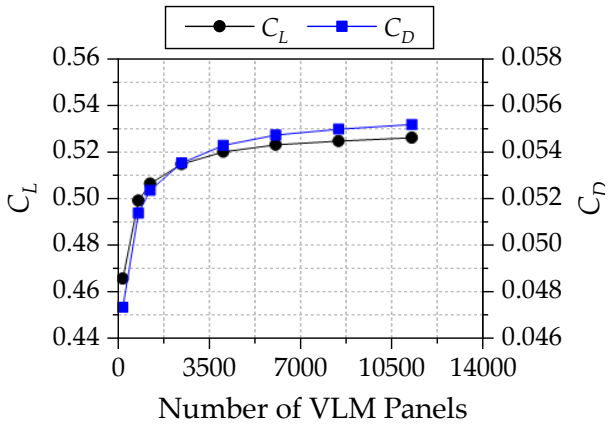

Figure 3. The variation in lift and drag coefficients with the number of VLM panels

2.3. Surrogate Model Generation using Response Surface Method

The Design of Experiment (DoE) method is a statistical approach used to generate and analyse controlled experiments to identify significant factors and optimize a process or system with minimal experimental effort. There are various types of DoE, such as Full Factorial Design, Plackett–Burman Design, Response Surface Method, Taguchi Design, and Latin Square Design [18].

Response Surface Method offers several key advantages for optimizing and evaluating nonlinear complex relationships. Compared with a full factorial design, RSM can fit the same model with fewer experiments and identify the optimal combination of input factors to achieve the desired outputs. Furthermore, RSM includes quadratic (curved) terms, allowing it to model curved or complex surfaces and capture not only main effects but also interactions among the

variables under investigation. There are various options in RSM, with the Central Composite Design (CCD) and the Box-Behnken Design (BBD) being the most common. While CCD is more flexible with an adjustable number of centre and axial points, BBD is more efficient for a small number of factors; however, it becomes more expensive at higher numbers. Detailed information about the methodology could be found in [19, 20].

In this manuscript, RSM analysis is to be performed in the commercially available Minitab software [21] to generate a surrogate model, a mathematical equation using variables G, S, and δ, capable of estimating C_L/C_D and $C_L^{3/2}/C_D$ values. For this purpose, CCD is applied to evaluate more extensive scenarios, including those beyond the constraints presented in Table 1. The gap distance was limited from 0.25*c* to 1.25*c*, while the stagger was from -*c* to *c*, where *c* is the chord length. The limits are defined to fully cover potential critical aerodynamic interactions, such as inter-wing interactions and monoplane-like behaviour, based on similar studies in the literature [22, 23]. The designed experiments are presented in Table 2, in which all variables exceed the constraints, enabling estimation of a broader range of configurations.

Table 1. Design constraints in RSM analysis

	Gap [*m*]	Stagger [*m*]	Decalage [*degrees*]
Minimum value	0.0381	-0.1524	-6
Maximum value	0.1905	0.1524	6

Table 2. Designed experiments for RSM-analysis

Number of Experiments	Gap [m]	Stagger [m]	Decalage [degrees]
1	0.248487	0	0
2	0.195	-0.1524	-6
3	0.11655	0	0
4	-0.015387	0	0
5	0.11655	0	0
6	0.195	0.1524	-6
7	0.0381	0.1524	6
8	0.11655	0	10.0908
9	0.11655	0	0
10	0.11655	0.256305	0
11	0.0381	0.1524	-6
12	0.0381	-0.1524	6
13	0.11655	0	0
14	0.11655	-0.256305	0
15	0.11655	0	0
16	0.11655	0	0
17	0.0381	-0.1524	-6
18	0.11655	0	-10.0908
19	0.195	0.1524	6
20	0.195	-0.1524	6

2.4. Genetic Algorithm for Optimization

Genetic Algorithm (GA) is a population-based, stochastic search method inspired by the principles of natural selection and genetics. It is particularly effective for solving nonlinear, multimodal, and complex optimization problems for which gradient-based methods are less effective or inapplicable. In this study, a Genetic Algorithm (GA) was employed to optimize the objective functions with respect to performance parameters related to the lift and drag coefficients. Further information on the algorithm's theoretical background is provided in [24].

In our case, the variables gap, stagger, and decalage were to be optimally selected, with the objective function defined as the maximization of C_L/C_D and $C_L^{3/2}/C_D$ separately, using the surrogate model generated via RSM. These aerodynamic parameters are directly proportional and crucially determine the range (R) and endurance (E) of piston-propelled aerial vehicles. The equations were given in Eq. (2) and Eq. (3), where η is the propulsive efficiency, SFC is the specific fuel consumption, ρ is the air density, S is the wing area, and W is the weight [24].

$$R = \frac{\eta}{SFC}\frac{C_L}{C_D}\ln\left(\frac{W_{initial}}{W_{final}}\right) \tag{2}$$

$$E = \frac{2}{SFC_t}\frac{{C_L}^{3/2}}{C_D}\sqrt{2\rho S}\ln\left({W_{final}}^{-1/2} - {W_{initial}}^{-1/2}\right) \tag{3}$$

The constraints were defined to conserve or enhance the lift coefficient relative to the base model, thereby providing adequate lift while improving performance, as given in Equations (4), (5), and (6).

$$C_{L_{base}} \leq C_{L_{optimal}} \tag{4}$$

$$\left(\frac{C_L}{C_D}\right)_{base} \leq \left(\frac{C_L}{C_D}\right)_{optimal} \tag{5}$$

$$\left(\frac{{C_L}^{3/2}}{C_D}\right)_{base} \leq \left(\frac{{C_L}^{3/2}}{C_D}\right)_{optimal} \tag{6}$$

The optimization process begins by generating an initial population of potential solutions (individuals), with each individual represented by a chromosome encoding a candidate solution to the problem. The algorithm was iterated in MATLAB until a termination criterion was met, either a fixed number of generations or a convergence threshold based on changes in fitness.

3. RESULTS AND DISCUSSION

3.1. RSM Analysis Results and Surrogate Models

The Pareto diagrams are illustrated in Fig. 4a and 4b, which present the relative importance of factors and interactions in affecting the responses C_L/C_D and $C_L^{3/2}/C_D$, respectively. From a lift-to-drag ratio perspective, the stagger has a minimal, nonlinear effect, whereas decalage has both linear and nonlinear strong effects on the response. In the case of $C_L^{3/2}/C_D$, stagger has only a dependent effect, interacting with decalage, while gap distance and decalage have a dramatic impact on the response.

The R-square (R^2), R-squared adjusted (R^2-adj), and R-squared predicted (R^2-pred) values in Table 3 indicate the model's predictive capability. Moreover, the p-values in Table 4 indicate the separate and combined effects of factors on the objective functions, with small p-values (typically ≤ 0.05) providing strong evidence against the null hypothesis. The results showed that the stagger and the interaction terms GS and $G\delta$ had no significant effect on either objective function. The terms δ^2 and S^2 have a slight effect on the lift-to-drag ratio and $C_L^{3/2}/C_D$, respectively, while S^2 has no considerable effect on $C_L^{3/2}/C_D$.

https://doi.org/10.31436/iiumej.v27i1.3980

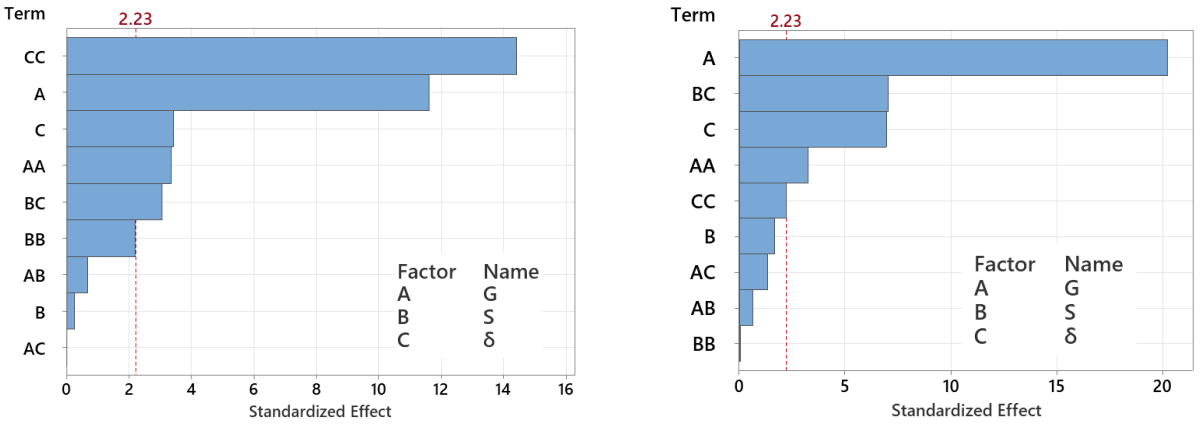

(a) (b)

Figure 4. a) Pareto diagram for C_L/C_D, b) Pareto diagram for $C_L^{3/2}/C_D$

Table 3. The model summary

Objective Functions	R^2	R^2-adj	R^2-pred
C_L/C_D	97.35%	94.97%	79.93%
$C_L^{3/2}/C_D$	98.14%	96.46%	83.79%

Table 4. The probability characteristics of variables

	P-values for Responses	
Parameters	C_L/C_D	$C_L^{3/2}/C_D$
G	0.000	0.000
S	0.799	0.125
δ	0.006	0.000
G^2	0.007	0.009
S^2	0.052	0.949
δ^2	0.000	0.051
GS	0.515	0.527
Gδ	0.985	0.208
Sδ	0.012	0.000

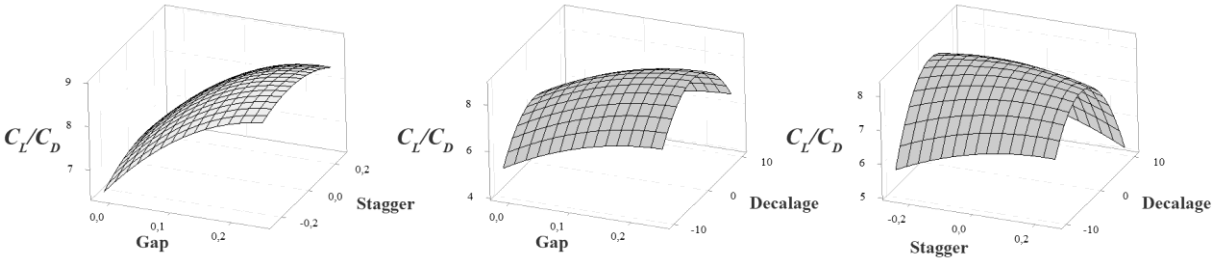

(a) (b) (c)

Figure 5. a) The response surface plot for gap and stagger for C_L/C_D, b) The response surface plot for gap and decalage for C_L/C_D, c) The response surface plot for stagger and decalage for C_L/C_D

The response surface plots for C_L/C_D and $C_L^{3/2}/C_D$ are shown in Fig. 5 and visually depict the relationships between the two independent variables and the response variables. In Fig. 5a, the maximum lift-to-drag ratio was clearly enhanced by increasing gap distance, while stagger had nearly no effect, parallel with its p-value. Similarly, in Fig. 5b, the larger gap distance contributed to the lift-to-drag ratio, whereas decalage required a moderate value to achieve this

improvement. Fig. 5c represented the slight effect of stagger on enhancing the lift-to-drag ratio, where decalage should be conserved moderately.

As shown in Fig. 6a, the graph was significantly dependent on the gap value, as indicated by the reported p-values. Similarly, in Fig. 6b, the increased gap distance was attributed to $C_L^{3/2}/C_D$, while a minimal effect was observed for the decalage. Fig. 6c showed that, for a smaller stagger, a higher decalage was required to enhance $C_L^{3/2}/C_D$.

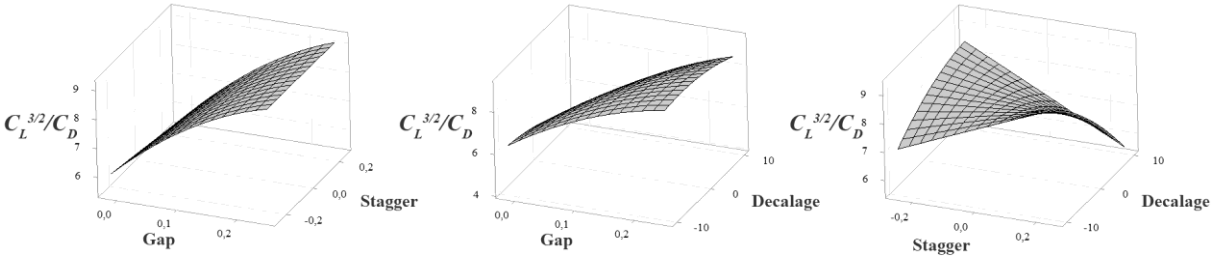

(a) (b) (c)

Figure. 6. a) The response surface plot for gap and stagger for $C_L^{3/2}/C_D$, b) The response surface plot for gap and decalage for $C_L^{3/2}/C_D$, c) The response surface plot for stagger and decalage for $C_L^{3/2}/C_D$

The surrogate models generated via RSM regression are shown in Eqs. (7) and (8) for each aerodynamic performance parameter, as functions of the variables G, S, and δ. Terms with p-values < 0.05 were removed from the models to simplify them.

$$\frac{C_L}{C_D} = 7.061 + 13.39G - 0.0285\delta - 26.21G^2 - 4.55S^2 - 0.01919\delta^2 - 0.2148S\delta \quad (7)$$

$$\frac{{C_L}^{3/2}}{C_D} = 6.077 + 18.66G - 0.0786\delta - 25.47G^2 - 0.00295\delta^2 - 0.4959S\delta \quad (8)$$

The predictions from the surrogate model were validated, and the results were compared with the designed experiments shown in Fig. 7, yielding satisfactory R2 values. The average difference between the regression predictions and analysis results were 0.0015% and 0.0441%, while the maximum differences were 3.52% and -5.76% for C_L/C_D and $C_L^{3/2}/C_D$, respectively.

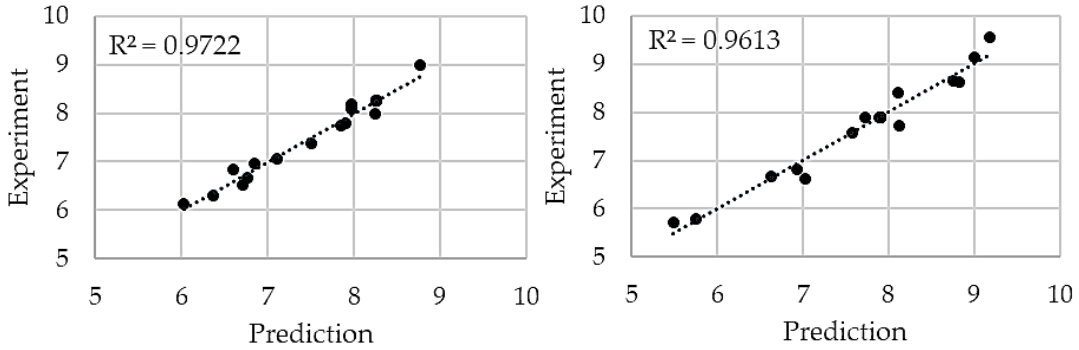

(a) (b)

Figure 7. a) Designed experiment results and surrogate model predictions for C_L/C_D, b) Designed experiment results and surrogate model predictions for $C_L^{3/2}/C_D$

3.2. Optimization Results

The base biplane model is determined to have no decalage or stagger, while having a gap distance of 0.5c. The upper and lower limits of the optimization algorithm were determined as values given in Table 5, where a maximum gap of one chord length was imposed due to

https://doi.org/10.31436/iiumej.v27i1.3980

structural considerations, and the decalage angle was limited to positive and negative six degrees to avoid stall onset.

The results of the genetic algorithm optimization are presented in Table 6, along with those of the base model. To maximize the lift-to-drag ratio, the algorithm increased the gap distance, as shown in the Pareto diagram, while applying moderate stagger and a slight negative decalage. In the case of $C_L^{3/2}/C_D$, the gap distance and stagger are maximized, while decalage is minimized within the limits.

Table 5. The constraints defined in the genetic algorithm

	***G* [*m*]**	***S* [*m*]**	***δ* [*degrees*]**
Minimum value	0	-0.3	-6
Maximum value	0.152	0.3	6

Table 6. The base and optimal configurations

Model	**Variable**				
	***G* [*m*]**	***S* [*m*]**	***δ* [*degrees*]**	C_L/C_D	$C_L^{3/2}/C_D$
Base	0.075	0	0	7.872	7.299
***Max.* C_L/C_D**	0.2554	0.02	-0.8557	8.7833	9.254
***Max.* $C_L^{3/2}/C_D$**	0.3664	0.3	-6	8.402	10.7527

The results indicated that a greater gap distance contributes to both range and endurance by reducing wing-to-wing interaction. Similarly, higher stagger values are associated with greater endurance. Correspondingly, optimization results favor higher gap and stagger values to minimize the adverse aerodynamic interference between the wings. Ideally, eliminating this interference would reveal the monoplane's efficiency. However, the justification for the biplane configuration in this study is driven by geometric and structural constraints, specifically the restriction on wing span for mini-UAV applications. To achieve the required wing loading and lift capacity within a confined span, a monoplane would require a significantly larger chord, resulting in a low Aspect Ratio and high induced drag. The biplane configuration addresses this problem, providing twice the lifting-surface area within the same span constraint while maintaining a higher effective aspect ratio than a comparable monoplane.

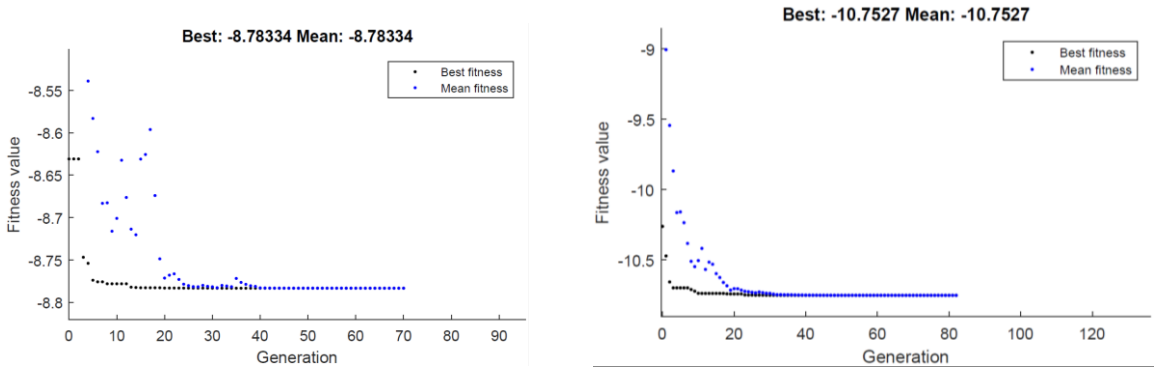

(a) (b)

Figure. 8. The variation in fitness value with number of generations for C_L/C_D, b) The variation in fitness value with number of generations for $C_L^{3/2}/C_D$

The base C_L/C_D and $C_L^{3/2}/C_D$ values were improved by 10.93% and 46.63%, respectively, according to surrogate-model-based optimization results, which are validated in the following section. The iterative optimization process is shown in Fig. 8, where fitness values are plotted against the number of generations.

3.3. Validation of the Optimal Configuration

The validity of the surrogate-model-based optimization results was assessed by aerodynamic analyses of each optimal configuration. The results are presented in Table 7, where the differences between surrogate model predictions and VLM analyses for C_L/C_D and $C_L^{3/2}/C_D$ were 2.17% and -8.36%, respectively, for optimal configurations. The maximum-range and maximum-endurance models have lift coefficients of 1.048 and 1.375, respectively, which are higher than the base model's 0.86, as intended.

Table 7. The base and optimal configurations

Model	Surrogate Model Prediction		VLM	
	C_L/C_D	$C_L^{3/2}/C_D$	C_L/C_D	$C_L^{3/2}/C_D$
Base	7.917	7.333	7.872	7.299
***Max.* C_L/C_D**	8.783	9.254	8.974	8.894
***Max.* $C_L^{3/2}/C_D$**	7.905	10.752	8.402	9.854

4. CONCLUSIONS

The present study focused on surrogate-model-based aerodynamic optimization of a piston-propelled mini biplane UAV wing to maximize the vehicle's range and endurance. Initially, the aerodynamic analysis method was validated on an existing monoplane wing design and compared with wind-tunnel results in the literature. Subsequently, a base biplane model was constructed, and the effects of multi-wing geometric parameters, namely decalage and stagger, were investigated. The gap distance was investigated using a central composite design in RSM, and surrogate models for estimating C_L/C_D and $C_L^{3/2}/C_D$ were developed. The surrogate model equations were simplified using Pareto analysis and incorporated into a genetic algorithm to obtain optimal sets of decalage, stagger, and gap distances that maximize range and endurance. Finally, the results from the surrogate model were compared with those from VLM analyses, yielding differences of 2.17% and -8.36% for C_L/C_D and $C_L^{3/2}/C_D$, respectively. The total improvement in C_L/C_D and $C_L^{3/2}/C_D$ values was 10.93% and 46.63%, respectively. Although the study has presented the aerodynamic effects of the design variables and provided optimal designs within the constraints, the structural limitations should be evaluated, particularly when significant gaps and stagger values are considered alongside aerodynamic considerations, to achieve more efficient optimization in a subsequent study.

REFERENCES

[1] Guo T, Feng L, Zhu C, Zhou X, Chen H. (2022) Conceptual Research on a Mono-Biplane Aerodynamics-Driven Morphing Aircraft. Aerospace, 9(7):380. https://doi.org/10.3390/aerospace9070380.

[2] Nguyen TD, Kashitani M, Taguchi M, Kusunose K. (2022) Effect of Stagger on Low-Speed Performance of Busemann Biplane Airfoil. Aerospace, 9(4):197. https://doi.org/10.3390/aerospace9040197.

[3] Guo R, Bai Y, Pei X, Lai Z. (2021) Numerical investigation of aerodynamics and wake on biplane airfoils at high angles of attack. International Journal of Mechanical Sciences, 205:106606. https://doi.org/10.1016/j.ijmecsci.2021.106606.

[4] Leifsson L, Koziel S, Tesfahunegn YA. (2016) Multiobjective aerodynamic optimization by variable-fidelity models and response surface surrogates. AIAA Journal, 54(2):531–541. https://doi.org/10.2514/1.J054128.

[5] Immonen E. (2017) 2D shape optimization under proximity constraints by CFD and response surface methodology. Applied Mathematical Modelling, 41:508–529. https://doi.org/10.1016/j.apm.2016.09.009.

[6] Tang X, Luo J, Liu F. (2017) Aerodynamic shape optimization of a transonic fan by an adjoint-response surface method. Aerospace Science and Technology, 68:26–36. https://doi.org/10.1016/j.ast.2017.05.005.

[7] Aelaei M, Karimian S, Ommi F. (2019) Sensitivity analysis and optimization of delta wing design parameters using CFD-based response surface method. Journal of Applied Fluid Mechanics, 12(6):1885–1903. https://doi.org/10.29252/jafm.12.06.29706.

[8] Tian-tian Z, Mohamed E, Wei H, Zhen-guo W, Derek BI, Lin M, Mohamed P. (2019) Winglet design for vertical axis wind turbines based on a design of experiment and CFD approach. Energy Conversion and Management, 195:712–726. https://doi.org/10.1016/j.enconman.2019.05.055.

[9] Yao X, Liu W, Han W, Li G, Ma Q. (2020) Development of response surface model of endurance time and structural parameter optimization for a tailsitter UAV. Sensors, 20(6):1766. https://doi.org/10.3390/s20061766.

[10] Hariharan K, Jun SL, Foster KK, Man YH, June KM. (2021) A multi-objective airfoil shape optimization study using mesh morphing and response surface method. Journal of Mechanical Science and Technology, 35:1075–1086. https://doi.org/10.1007/s12206-021-0221-0.

[11] Win SY, Thianwiboon M. (2021) Parametric optimization of NACA 4412 airfoil in ground effect using full factorial design of experiment. Engineering Journal, 25(12):9–19. https://doi.org/10.4186/ej.2021.25.12.9.

[12] Yildirim BY, Tuncer H. (2021) Wing planform optimization using flow solutions and response surface methodology. AIAA Aviation Forum, p.2564. https://doi.org/10.2514/6.2021-2564.

[13] Simmons BM. (2023) Evaluation of response surface experiment designs for distributed propulsion aircraft aero-propulsive modelling. AIAA SciTech Forum, p.2551. https://doi.org/10.2514/6.2023-2251.

[14] Dam B, Pirasaci T, Kaya M. (2022) Artificial neural network based wing planform aerodynamic optimization. Aircraft Engineering and Aerospace Technology, 94(10):1731–1747. https://doi.org/10.1108/AEAT-10-2021-0311.

[15] Samputh HH, Moey LK, Tai VC, Tan YC. (2024) Investigation of aerodynamic characteristics of swept C-wing configurations at transonic speed using design of experiments and computational fluid dynamics. Aviation, 28(2):72–84. https://doi.org/10.3846/aviation.2024.21495.

[16] Analysis of foils and wings operating at low Reynolds numbers. (2025) Available at: https://aero.us.es/adesign/Slides/Extra/Aerodynamics/Software/XFLR5/XFLR5%20v6.10.02/Guidelines.pdf (Accessed 19 July 2025).

[17] Bastedo WG, Mueller TJ. (1986) Spanwise variation of laminar separation bubbles on wings at low Reynolds number. Journal of Aircraft, 23(9):687–694. https://doi.org/10.2514/3.45363.

[18] Durakovic B. (2017) Design of experiments application, concepts, examples: State of the art. Periodicals of Engineering and Natural Sciences, 5(3):421-439. https://doi.org/10.21533/pen.v5i3.145.

[19] Myers RH, Montgomery DC. (1996) Response Surface Methodology. Taylor and Francis, USA.

[20] Antony J. (2023) Design of Experiments for Engineers and Scientists. Elsevier, UK.

[21] Alin A. (2010) Minitab. Wiley Interdisciplinary Reviews: Computational Statistics, 2(6):723–727. https://doi.org/10.1002/wics.113.

[22] Jones R., Cleaver D.J., Gursul I. (2015) Aerodynamics of biplane and tandem wings at low Reynolds numbers. Exp Fluids, 56: 124. https://doi.org/10.1007/s00348-015-1998-3.

[23] Cai Y., Liu G., Zhu X., Tu Q., Hong G. (2019) Aerodynamic interference significance analysis of two-dimensional front wing and rear wing airfoils with stagger and gap variations. Journal of Aerospace Engineering, 32(6): 04019098. https://doi.org/10.1061/(ASCE)AS.1943-5525.0001090.

[24] Şumnu A, Eraslan Y. (2025) Aerodynamic shape optimization of simplified ground vehicle (Ahmed Body) using passive control devices. Mechanics, 31(1):5–14. https://doi.org/10.5755/j02.mech.36452.

[25] Pogosyan MA. (2025) Aircraft Design. Springer Nature. https://doi.org/10.1007/978-981-96-4599-2.